THE CRACK PROBLEM FOR AN ORTHOTROPIC HALF PLANE STIFFENED BY ELASTIC FILMS

by

R. Mahajan, F. Erdogan and Y.T. Chou

Lehigh University, Bethlehem, PA

August 1992

FINAL PROJECT REPORT

OFFICE OF NAVAL RESEARCH CONTRACT NO. NOOO14-89-3188

THE CRACK PROBLEM FOR AN ORTHOTROPIC HALF PLANE STIFFENED BY ELASTIC FILMS

by

R. Mahajan, F. Erdogan and Y.T. Chou

Lehigh University, Bethlehem, PA

August 1992

FINAL PROJECT REPORT

OFFICE OF NAVAL RESEARCH CONTRACT NO. N000014-89-3188

St-A per telecom, Mr. Rajatakse,
ONR/Code 1132sm, Arl., VA.
JK 10-16-92

THE CRACK PROBLEM FOR AN ORTHOTROPIC HALF-PLANE STIFFENED BY ELASTIC FILMS

Ravi Mahajan
Department of Mechanical Engineering and Mechanics

F. Erdogan
Department of Mechanical Engineering and Mechanics

Y. T. Chou
Department of Materials Science and Engineering, Lehigh University,
Bethlehem, PA 18015.

ABSTRACT

In this paper, various contact and crack problems for an orthotropic substrate, stiffened by elastic films, are considered. The film is modeled as a membrane and the substrate as an orthotropic half-plane with the principal axes of orthotropy parallel and perpendicular to the boundary. The problem is formulated in terms of a system of singular integral equations. Various asymptotic analyses are carried out in order to determine the nature of the stress singularities. The special cases for which the solution is obtained and results are provided include the stiffened half-plane without the crack, the cracked half-plane without any stiffeners, the orthotropic half-plane with a single stiffener and a crack emanating from the endpoint of the stiffener, and a broken stiffener on a cracked half-plane. In each case the influence of the relative crack/stiffener dimensions, the film/substrate stiffness ratios, and the material orthotropy on the stress intensity factors is studied and some sample results are given.

1. Introduction

The problem of stress concentrations caused by thin, elastic film overlays on substrates has attracted a great deal of attention in recent years because of its importance in a number of microelectronics, optical and structural applications. The edges of these films are known to be regions of stress concentration [1, 2], the stresses being produced by processing, thermal mismatch or mechanical and thermal loading. The investigation of the related stress analysis problem is essential for understanding

the associated physical effects such as dislocation generation, film debonding and film and substrate distortion and cracking. It is further known that especially for applications in microelectronics and composites, both the film and the substrate demonstrate significant anisotropy in their elastic properties [3]. This anisotropy must be taken into account while studying the mechanics of the film-substrate composite medium.

Among the early studies of the problem of a film bonded to an elastic substrate one may mention those by Arutiunian[4, 5] who formulated the problem in terms of a singular integral equation. In [4] the problem of a single film and in [5] the interaction of periodically spaced films was considered. A simpler formulation of the same problem including the interaction of multiple stiffeners was considered by Erdogan[6]. In the solutions given in [4]-[6], the film was assumed to be very thin and hence the effect of bending stiffness and the variation of stresses through film thickness was neglected. Thus, the film was modeled as a membrane and the only contact stress was the interfacial shear stress. In [6] a simple and efficient numerical technique incorporating the correct form of the stress singularities was used to solve the resulting integral equation. Once the shear stress on the interface was determined, the stresses in both the film and the substrate were easily calculated. It was shown that the contact shear stress had a square root singularity having a Mode-II stress intensity factor. The magnitude of this stress intensity factor was shown to depend on a stiffness parameter that is a measure of the relative stiffnesses of the half-plane and the film. Erdogan and Gupta[7] considered the single stiffener problem and studied the regularity of the solution in terms of the stiffness parameter. Delale and Erdogan[8] used these solutions to study the associated failure problem. The membrane stiffener problem has also been studied recently by Erdogan and Joseph[9] who gave a detailed asymptotic analysis of the singular behavior of the solution for an arbitrary membrane-substrate contact angle and showed that the power of the stress singularity varies between 0 and 1/2 as the contact angle varies between 0 and 90 degrees.

In the present study, the contact stress problem for elastic films directly bonded to an orthotropic substrate containing a crack is considered. In general, depending on their relative dimensions, the film and the substrate can be modeled as membranes, plates or half-planes [6, 10, 11]. The main thrust of this paper is towards applications where the dimensions of the substrate are considerably greater than that of the film and hence the substrate may be modeled as a half-plane and the film as a membrane. The effect of material anisotropy is taken into account by assuming both the film and the substrate as being orthotropic. The general problem is formulated in terms of a system

of singular integral equations which are solved for various film and crack geometries. A particular emphasis is placed on the surface crack in the substrate initiating at the film end.

2. The General Formulation of the Problem

Consider the plane elasticity problem for an orthotropic half-plane stiffened by a number of membranes and containing a crack (see, for example Figures 1 and 2). The problem may easily be formulated by using the solutions for a pair of dislocations in the half-plane and a pair of concentrated forces acting on the boundary as the Green's functions. Let the half-plane contain a pair of dislocations at a point (x_1, y_1) having the components of the Burgers vector f_1 and f_2 parallel and perpendicular to the boundary, respectively. The stresses at a point (x, y) in the half-plane due to these dislocations may be expressed as

$$\begin{aligned}
\sigma_{11}(x, y; x_1, y_1) &= K_{11}(x, y, x_1, y_1) f_1 + K_{12}(x, y, x_1, y_1) f_2, \\
\sigma_{12}(x, y; x_1, y_1) &= K_{21}(x, y, x_1, y_1) f_1 + K_{22}(x, y, x_1, y_1) f_2, \\
\sigma_{22}(x, y; x_1, y_1) &= K_{31}(x, y, x_1, y_1) f_1 + K_{32}(x, y, x_1, y_1) f_2,
\end{aligned} \tag{1}$$

where the functions K_{ij} $(i = 1, 2, 3, j = 1,2)$ are given in Appendix A (see [12]).

Similarly, the stresses in an orthotropic half-plane due to the boundary tractions

$$\sigma_{12}(0, y) = f_3\,\delta(y - y_o), \sigma_{11}(0, y) = f_4\,\delta(y - y_o), \tag{2}$$

are given by

$$\begin{aligned}
\sigma_{11}(x, y; y_o) &= K_{13}(x, y, y_o) f_3 + K_{14}(x, y, y_o) f_4, \\
\sigma_{12}(x, y; y_o) &= K_{23}(x, y, y_o) f_3 + K_{24}(x, y, y_o) f_4, \\
\sigma_{22}(x, y; y_o) &= K_{33}(x, y, y_o) f_3 + K_{34}(x, y, y_o) f_4.
\end{aligned} \tag{3}$$

where the functions K_{ij}, $(i = 1, 2, 3$ and $j = 3, 4)$ are also given in Appendix A[13].

The functions K_{ij} contain the parameter C_h defined by (A12) which characterizes the anisotropy of the substrate. It was shown by Chou[14] that C_h has a range between -4 and ∞. Physically, $C_h = 0$ corresponds to an isotropic material. It was further

demonstrated that the sign of C_h has an important influence on the analysis of stress fields. It turns out that the roots of the characteristic equation resulting from the solution of the equilibrium equations for the plane orthotropic medium are real for $C_h > 0$ and complex for $C_h < 0$. The formulation considered here is valid for all values of C_h. It should be noted that the constant C_h is essentially the same as the orthotropy parameter κ defined in [15] and [16] ($C_h = 2\ (\kappa - 1)$, see [17] for discussion). In this paper numerical results are presented for six different materials having the elastic constants listed in Table 1. Materials 1 and 2 are fiber-reinforced composites. Material 3 is isotropic. Material 4 with $C_h = -0.0022$ is nearly isotropic and is included largely to verify the numerical procedure developed for orthotropic materials. Materials 5 and 6 are Silicon and Gallium Arsenide, respectively.

Since the bending stiffness of the film is assumed to be negligible, it may be modelled by a membrane in which the stress component σ_{11} vanishes, σ_{22} is independent of the thickness coordinate and the distributed interfacial shear stress $\sigma_{12} = f_3(y)$ may be treated as a body force. Thus we may assume that in (2) and (3) $f_4 = 0$ and the crack-contact problem described, for example, in Fig.1 may be formulated by considering f_1, f_2 and f_3 as continuously distributed functions that satisfy the appropriate continuity and equilibrium conditions. The continuity of displacements along the film-substrate interface requires that

$$\frac{\partial}{\partial y} v_1(y) \;=\; \frac{\partial}{\partial y} v_2(0, y), \quad a_i < y < b_i, \quad i = 1,.., n \tag{4}$$

where v_1 and v_2 are the y-components of the displacements in the film and the substrate respectively, a_i and b_i refer to the film ends, and without any loss in generality the continuity condition is expressed in differentiated form.

If we now designate the stress state in the half-plane by σ_{xx}, σ_{xy}, σ_{yy}, and define the coordinate system (s, n) shown in Fig.1, the remaining conditions refer to the fact that the crack surfaces are traction-free, that is

$$\sigma_{nn}(s) \;=\; \sigma \;\; sin^2\theta \;+\; \sigma_{yy}\, cos^2\theta \;-\; \sigma_{xy}\, sin2\theta \;=\; 0, (A < s < B), \tag{5}$$

$$\sigma_{sn}(s) \;=\; (\sigma_{yy} - \sigma_{xx})\, cos\theta\, sin\theta + \sigma_{xy}\, cos2\theta \;\;=\;\; 0, (A < s < B), \tag{6}$$

By observing that $\partial v/\partial y = \epsilon_{yy}$ and that f_3 is the only applied force acting on the film, from the equilibrium of the film it may easily be shown that

$$\frac{\partial}{\partial y} v_1(y) \;=\; -\frac{\beta_{22}^1}{h} \int_{a_i}^{y} f_3(y_o)\, dy_o\,, \;\; (a_i < y < b_i),\; i = 1, .., n, \tag{7}$$

where the film is assumed to be orthotropic having the stiffness coefficients C_{ij}^1 and β_{22}^1 is defined by[1]

$$\beta_{22}^{1} \;=\; \frac{C_{11}^1}{\left\{C_{11}^1\; C_{22}^1\; -\left(C_{12}^1\right)^2\right\}}. \tag{8}$$

Similarly, on the boundary of the half-plane from (1), (3) and $\sigma_{xx}(0,\, y) = 0$, $\sigma_{xy}(0,\, y) = f_3(y)$ it may be shown that

$$\frac{\partial}{\partial y} v_2(0,\, y) \;=\; \beta_{22} \left\{\sigma_o + \int_A^B K_{31}(0,\, y;\, x_1,\, y_1)\, f_1(t)\, dt \right.$$
$$\left. + \int_A^B K_{32}(0,\, y;\, x_1,\, y_1)\, f_2(t)\, dt + \sum_{i=1}^{n} \int_{a_i}^{b_i} K_{33}(0,\, y,\, y_o)\, f_{3i}(y_o)\, dy_o \right\}, \tag{9}$$

where

$$\sigma_o \;=\; \sigma_{yy}(x,\, \pm\infty), \tag{10}$$

$$x \;=\; s\, cos\theta,\; y \;=\; s\, sin\theta,\; x_1 \;=\; t\, cos\theta,\; y_1 \;=\; t\, sin\theta, \tag{11}$$

$$\beta_{22} \;=\; \frac{C_{11}}{\left\{C_{11}\; C_{22}\; -(C_{12})^2\right\}}, \tag{12}$$

C_{ij} being the stiffness coefficients of the half-plane (see Appendix A). In solving the problem it is assumed that the substrate is subjected to uniform tension $\sigma_{yy} = \sigma_o$ away from the film-crack region. Other simple forms of practical loading may be uniform temperature changes and residual stresses which may be interpreted in terms of a constant strain mismatch along the film-substrate interface. Observing that σ_o is the only external load amplitude, it may easily be considered as being also a measure of the strain mismatch on the interface[9].

Substituting from (1), (3), (7) and (9) into (4)-(6) we obtain a system of integral equations for the unknown functions f_1, f_2 and f_{3i}, where f_{3i} is the interface shear for the ith film, (i = 1,..., n). The conditions of equilibrium of the films and the single-valuedness of the displacements require that the solution of the integral equations be

[1] β_{ij} and β_{ij}^1 are the coefficients of the compliance matrix for the substrate and the film, respectively.

subject to

$$\int_{a_i}^{b_i} f_{3i}(y_o)\, dy_o = 0,\ i = 1, 2, ..., n, \tag{13}$$

$$\int_{A}^{B} f_1(t)\, dt = 0,\ \int_{A}^{B} f_2(t)\, dt = 0. \tag{14}$$

3. The Integral Equations

In materials stiffened by elastic membranes the endpoints of the stiffener are known to be points of singularity. Thus, aside from the cracking of the membrane due to high tensile stresses, the most likely modes of failure in the bonded medium appear to be debonding along the interface and crack initiation and propagation in the substrate around the singular points. With the membrane model, debonding may be interpreted simply as the shortening of the film and, therefore, does not require any new concepts and analysis. Cracking of the substrate normally requires the solution of the problem for a crack growing radially from the singular point (Fig.1, $A = 0$, $\theta = \theta_{cr}$). The direction of the crack growth must be determined by maximizing the ratio of the strain energy release rate to the fracture toughness. Since the material is orthotropic, in the problem under consideration, both of these quantities are dependent on θ and θ_{cr} and may not be determined without the full fracture toughness characterization of the orthotropic medium. However, in orthotropic materials the principal planes of orthotropy are also known to be the weak cleavage planes. Furthermore, under the Mode-II conditions prevailing around the film end for $-30^{\circ} < \theta < 30^{\circ}$ (where θ_{cr} falls) the θ variation of the strain energy release rate is relatively weak. It is, therefore, safe to assume that in the film problem considered $\theta = 0$ is by far the most likely fracture plane (Fig.1).

By substituting $\theta = 0$, from (5), (6) and (4) it may then be shown that

$$\frac{1}{\pi}\int_c^d \frac{f_1(t)}{t-x}\, dt + \int_c^d N_{11}(x, t)\, f_1(t)\, dt + \int_c^d N_{12}(x, t)\, f_2(t)\, dt + \sum_{i=1}^{n} \int_{a_i}^{b_i} N_{13}(x, y_o)\, f_{3i}(y_o)\, dy_o = g_1(x),\ (c < x < d), \tag{15}$$

$$\frac{1}{\pi}\int_c^d \frac{f_2(t)}{t-x}\, dt + \int_c^d N_{21}(x, t)\, f_1(t)\, dt + \int_c^d N_{22}(x, t)\, f_2(t)\, dt + \sum_{i=1}^{n} \int_{a_i}^{b_i} N_{23}(x, y_o)\, f_{3i}(y_o)\, dy_o = g_2(x),\ (c < x < d), \tag{16}$$

$$\sum_{i=1}^{n} \frac{1}{\pi} \int_{a_i}^{b_i} \frac{f_{3i}(y_o)}{y_o - y}\, dy_o + \int_c^d N_{31}(y,\, t) f_1(t)\, dt + \int_c^d N_{32}(y,\, t) f_2(t)\, dt + \int_{a_j}^{b_j} N_{33}(y,\, y_o) f_{3j}(y_o)\, dy_o$$

$$= \quad g_3(y),\ (a_j < y < b_j),\ (j = 1,..,\ n) \qquad (17)$$

where the Cauchy kernels and the Fredholm kernels N_{ij} follow from K_{ij} $(i,\, j = 1,\, 2,\, 3)$ given in Appendix A. Thus referring to Appendix A it may be shown that

$$N_{11}(x,\, t) \quad = \quad \frac{2}{\pi\, C_h} \left\{ \frac{(C_h + 4)}{2\,(x + t)} - \frac{\{2\, x + t\,(C_h + 2)\}}{\left\{ x^2 + (C_h + 2)\, x\, t + t^2 \right\}} \right\}, \qquad (18)$$

$$N_{12}(x,\, t) \quad = \quad 0, \qquad (19)$$

$$N_{13}(x,\, y_o) \quad = \quad \frac{2 \sqrt{(C_h + 4)}\, y_o^3\, \lambda^3}{\pi\, K_n \left\{ (y_o^2 + \lambda^2\, x^2)^2 + C_h\, x^2 \lambda^2 y_o^2 \right\}}, \qquad (20)$$

$$N_{21}(x,\, t) \quad = \quad 0, \qquad (21)$$

$$N_{22}(x,\, t) \quad = \quad N_{11}(x,\, t), \qquad (22)$$

$$N_{23}(x,\, y_o) \quad = \quad -\frac{2 \sqrt{(C_h + 4)}\, x\, y_o^2\, \lambda^3}{\pi\, K_n \left\{ (y_o^2 + \lambda^2\, x^2)^2 + C_h\, x^2 \lambda^2 y_o^2 \right\}}, \qquad (23)$$

$$N_{31}(y,\, t) \quad = \quad \frac{K_n (C_h + 4)^{\frac{3}{2}}\, t\, \lambda^3 y^2}{\pi \left\{ (t^2 + \lambda^2\, y^2)^2 + C_h\, y^2 \lambda^2 t^2 \right\}}, \qquad (24)$$

$$N_{32}(y,\, t) \quad = \quad -\frac{K_e (C_h + 4)^{\frac{3}{2}}\, \lambda\, t^2\, y}{\pi \left\{ (t^2 + \lambda^2\, y^2)^2 + C_h\, y^2 \lambda^2 t^2 \right\}}, \qquad (25)$$

$$N_{33}(y,\, y_o) \quad = \quad -\frac{\beta_{22}^1\ \lambda\, H(y - y_o)}{\beta_{22}\ h \sqrt{(C_h + 4)}}, \qquad (26)$$

$$g_1(x) \quad = \quad \frac{2\, \sigma_o}{K_n}, \qquad (27)$$

$$g_2(x) \quad = \quad 0, \qquad (28)$$

$$g_3(y) \quad = \quad \frac{\lambda\, \sigma_o}{\sqrt{(C_h + 4)}}, \qquad (29)$$

where $H(y - y_o)$ is the Heaviside function and the constants C_h, K_n, λ, and K_e are defined in Appendix A.

4. The Special Cases

In the special case of an orthotropic half-plane without any cracks and stiffened by a single membrane along $x = 0,\ -a < y < a$, the integral equations of the problem are reduced to

$$\frac{1}{\pi}\int_{-a}^{a}\frac{f_3(y_o)}{y_o - y}\,dy_o - \frac{\lambda\,\beta_{22}^1}{h\,\beta_{22}\sqrt{(C_h+4)}}\int_{-a}^{y} f_3(y_o)\,dy_o = \frac{\lambda\,\sigma_o}{\sqrt{(C_h+4)}} = \sigma_o, -a < y < a, \quad (30)$$

subject to

$$\int_{-a}^{a} f_3(y_o)\,dy_o = 0. \quad (31)$$

We now define

$$y_o = at,\ y = ar,\ \frac{\lambda\,\beta_{22}^1}{\beta_{22}\sqrt{(C_h+4)}}\left\{\frac{a}{h}\right\} = \lambda_s,\ \frac{f_3(y_o)}{\sigma_o'} = \sqrt{(1-t^2)}\sum_{n=0}^{\infty} A_n\,T_n(t). \quad (32)$$

By using the following results [9]

$$\frac{1}{\pi}\int_{-1}^{1}\frac{T_n(t)\,dt}{(t-r)\sqrt{1-t^2}} = \begin{cases} 0, & n = 0, \quad -1 < r < 1, \\ U_{n-1}(r), & n = 1, 2, \ldots, \quad -1 < r < 1, \\ -\dfrac{|r|/r}{\sqrt{r^2-1}}\left[r - (|r|/r)\sqrt{r^2-1}\right]^n, & n = 0,1, \ldots, \ |r| > 1 \end{cases} \quad (33)$$

$$\int_{-1}^{r} w(t)\,T_n(t)\,dt = -\frac{1}{n}\,U_{n-1}(r)\sqrt{1-r^2},\ n > 0, \quad (34)$$

and a method of collocation, (30) may be reduced to

$$\sum_{n=1}^{\infty} A_n\,U_{n-1}(r_i)\left\{1 + \frac{\lambda_s\sqrt{1-r_i^2}}{n}\right\} = 1,\ i = 1, 2, \ldots, \quad (35)$$

where $T_n(t)$ and $U_n(t)$ are the Chebychev polynomials of the first and second kind, respectively. The linear system (35) is solved by truncating the series at $n = N$ and by monitoring the convergence of the results. The selection of the collocation points r_i is, in general, arbitrary. It is known that good convergence is obtained by selecting more points near the ends[9]. For the present study, the collocation points are selected as

$$T_N(r_i) = 0,\ r_i = \cos\theta_i,\ \theta_i = \frac{(2\,i-1)\,\pi}{2\,N},\ (i = 1 \ldots N). \quad (36)$$

From (30) it may be seen that $f_3(y_o)$ has a form similar to the stress field due to a crack under pure Mode-II loading and, therefore, it is possible to define a stress intensity factor at the film edges as follows:

$$k_2(a) \;=\; \lim_{y \to a} \sqrt{2(a - y)}\, \sigma_{xy}(0, y). \tag{37}$$

The value of this stress intensity factor is dependent on the stiffness parameter λ_s which is proportional to the ratio of the stiffness of the substrate to the stiffness of the film in the y direction. Figure 3 shows the variation of the normalized stress intensity factor at the film edge as a function of λ_s. For $\lambda_s = 0$, that is, for an inextensible film, (30) has a closed-form solution [6] and the value of the normalized stress intensity factor is unity which is the upper bound. Similarly, from (30) and (32) it may be seen that as the stiffness of the film decreases (i.e., as $\lambda_s \to \infty$), the shear stress f_3 and, consequently the stress intensity factor k_2 tends to zero.

Once the shear stress in the contact region is determined, the tensile stress in the film may be obtained from the following relation

$$\sigma^1_{yy}(y) \;=\; -\frac{1}{h}\int_{-a}^{y} f_3(y_o)\, dy_o \;=\; \sigma_o\, a\, \frac{\sqrt{1 - (y/a)^2}}{h} \sum_{n=1}^{\infty} \frac{A_n U_{n-1}(y/a)}{n}. \tag{38}$$

A typical plot of this film stress is shown in Fig.4. It is seen that the maximum normal film stress is at the center of the film i.e. at $y = 0$. This implies that the $y = 0$ is the most likely site for potential film failure. Once the film fails completely in the center, a crack can propagate either along the interface or into the substrate. The latter case is a strong possibility as demonstrated in [6]. For the case of two stiffeners placed symmetrically with respect to the x-axis, it was shown that there was a "strong" singularity in the state of stress in the half-plane for the limiting case as the distance between the stiffeners approaches zero. Recognizing that complete film rupture represents this limiting case, one would expect that the crack would almost certainly propagate into the substrate or along the interfaces. This problem for the cracked substrate is considered in Section 6 of this paper.

The second special case which is of considerable practical interest is the case of a crack perpendicular to the boundary of a symmetrically loaded orthotropic half-plane without any stiffeners. In this case f_1 is the only unknown function and the integral equations (15)-(17) are reduced to

$$\frac{1}{\pi}\int_{c}^{d} \frac{f_1(t)}{t - x}\, dt + \int_{c}^{d} N(x, t)\, f_1(t)\, dt \;=\; \frac{2\,\sigma_2}{K_n} \;=\; \sigma_o\,, \quad (c < x < d), \tag{39}$$

where

$$N(x,\ t) \ = \frac{2}{\pi\ C_h}\left\{\frac{(C_h+4)}{2\ (x+t)} - \frac{\{2\ x+t\ (C_h+2)\}}{\left\{x^2+(C_h+2)\ x\ t+t^2\right\}}\right\}, \tag{40}$$

the dislocation density $f_1(t)$ is defined by

$$f_1(t) \ = \ -\ \frac{\partial}{\partial t}\{v_2(t,\ +0) \ -\ v_2(t,\ -0)\}, \tag{41}$$

and the constants K_n and C_h are given in Appendix A.

Note that for isotropic materials $C_h = 0$ and from (40) it may easily be shown that

$$\lim_{C_h \to 0}\ N(x,\ t,\ C_h) \ = \ \frac{1}{\pi}\left\{\frac{1}{(x+t)} + \frac{2\ t\ (x\ -\ t)}{(x+t)^3}\right\}, \tag{42}$$

which is the known result for an isotropic half-plane with a crack perpendicular to the boundary.

If $c > 0$, the function $f_1(t)$ must satisfy the following single-valuedness condition:

$$\int_c^d f_1(t)\ dt \ = \ 0. \tag{43}$$

The integral equation (39) may then be solved by following the procedure described previously in this section. After determining $f_1(t)$ the stress intensity factors may be defined by and evaluated from

$$k_1(d) \ = \ \lim_{x \to d}\sqrt{2(x\ -\ d)}\ \sigma_{yy}(x,\ 0) \ = \ +\lim_{x \to d}\frac{K_n}{2}\sqrt{2(d\ -\ x)}\ f_1(x), \tag{44}$$

$$k_1(c) \ = \ \lim_{x \to c}\sqrt{2(c\ -\ x)}\ \sigma_{yy}(x,\ 0) \ = -\lim_{x \to c}\frac{K_n}{2}\sqrt{2(x\ -\ c)}\ f_1(x). \tag{45}$$

From (39), (40) and (42), it may be observed that the kernel is independent of the elastic constants in the isotropic case, and depends only on a single dimensionless material constant C_h for orthotropic materials. The stiffness constants $K_n/2$ in (39) and $2\mu/(1+\kappa)$ in the isotropic case simply serve as scaling parameters for the crack opening displacement. Thus the stress intensity factors would be independent of the material constants in isotropic materials and would be a function of C_h only in orthotropic solids. The results for the internal crack problem are given in Table 2. From this table it may be seen that the stress intensity factors are monotonically decreasing functions of C_h

and the relative distance $\{ (d + c)/(d - c)\}$ from the surface. As $\{ (d + c)/(d - c)\} \rightarrow 1$, i.e. as $c \rightarrow 0$, $k_1(c)$ becomes unbounded (because of diminishing ligament size c) and $k_1(d)$ approaches the value given by the edge crack solution.

A second observation that is important in this problem concerns the effect of a 90-degree rotation in the axes of orthotropy. From the definition given by (A12), C_k is seen to be invariant with respect to a 90-degree material rotation. Hence the kernel of the integral equation and consequently the stress intensity factors would also remain invariant with respect to a 90-degree material rotation. Similar invariance has been previously observed by Delale and Erdogan[18] for the problem of an orthotropic strip with internal and edge cracks. This invariance is conditional in that the boundary conditions at $x = 0$ are required to be independent of the y-coordinate[18]. In the internal and edge crack problems involving membrane stiffners, where the boundary conditions depend on the y coordinate, it is shown that the stress intensity factors indeed vary with a 90-degree material rotation.

From its derivation it is clear that the integral equation (39) is valid for the edge crack as well as for the internal crack problem. However, for $c = 0$ it is seen that the kernel $N(s, t)$ becomes unbounded as $(x, t) \rightarrow 0$ simultaneously. Thus, apart from the Cauchy singularity, the equation contains a generalized Cauchy kernel which may have an effect on the behavior of the unknown function $f_1(t)$ at $t = 0$. This behavior may be examined quite simply by following a function-theoretic method [19]. For a sectionally holomorphic function $F(z)$ defined by the density function $f_1(t)$ as

$$F(z) = \frac{1}{\pi} \int_0^d \frac{f_1(t)}{t - z}\, dt, \tag{46}$$

assuming that

$$f_1(t) = \frac{\phi_1(t)}{t^{\beta}\,(d - t)^{\omega}}, \quad (0 < Re(\beta, \omega) < 1), \tag{47}$$

we have the following asymptotic expression [19]

$$F(z) = \frac{\phi_1(0)\, e^{i\beta\pi}}{d^{\omega}\, sin\beta\pi\, (z - c)^{\beta}} - \frac{\phi_1(d)}{d^{\beta}\, sin\omega\pi\, (z - d)^{\omega}} + F_o(z), \tag{48}$$

where $\phi_1(t)$ is bounded in $0 \leq t \leq d$ and nonzero at $t = 0$ and $t = d$, and $F_o(z)$ is either bounded or has singularities that are of lower order than that of $F(z)$. If we now express the kernel $N(x, t)$ in terms of the following partial fractions

$$N(x,\ t) \ = \ \frac{(p+2)}{C_k\,(t+x)} \ - \ \frac{2\,(2+p\,p_1)}{C_k(p_1\ -\ p_2)\,(t\ -\ p_1 x)}$$
$$+\ \frac{2\,(2+p\,p_2)}{C_k(p_1\ -\ p_2)\,(t\ -\ p_2 x)}, \tag{49}$$

$$p_{1,2} \ = \ \frac{-p\ \pm\ \sqrt{p^2\ -\ 4}}{2}, p \ = \ C_k + 2, \tag{50}$$

the integral equation (39) becomes

$$\frac{1}{\pi}\int_0^d \frac{f_1(t)}{t\ -\ x}\,dt + \frac{(p+2)}{C_k}\,\frac{1}{\pi}\int_0^d \frac{f_1(t)}{(t+x)}\,dt$$
$$-\ \frac{2\,(2+p\,p_1)}{C_k(p_1\ -\ p_2)}\,\frac{1}{\pi}\int_0^d \frac{f_1(t)}{(t\ -\ p_1 x)}\,dt$$
$$+\ \frac{2\,(2+p\,p_2)}{C_k(p_1\ -\ p_2)}\,\frac{1}{\pi}\int_0^d \frac{f_1(t)}{(t\ -\ p_2 x)}\,dt \ = \ \frac{2\,\sigma_o}{K_n},\ (0 < x < d). \tag{51}$$

Thus, from (48) and (51) it follows that

$$\frac{\phi_1(0)}{d^\omega x^\beta}\left\{cot\beta\pi + \frac{(p+2)}{C_k\,sin\beta\pi} - \frac{2\,(2+p\,p_1)\,e^{i\beta\pi}}{C_k(p_1\ -\ p_2)\,sin\beta\pi\ p_1^\beta}\right.$$
$$\left. + \frac{2\,(2+p\,p_2)\,e^{i\beta\pi}}{C_k(p_1\ -\ p_2)\,sin\beta\pi\ p_2^\beta}\right\} - \frac{\phi_1(d)}{d^\beta\,(d\ -x)^\omega}\,cot\omega\pi \ = \ \Theta(x), \tag{52}$$

where $\Theta(x)$ represents all lower order terms. Multiplying (52) by $(d\ -\ x)^\omega$ and taking the limit as $x \rightarrow d$ we obtain

$$\frac{\phi_1(d)}{d^\beta}\,cot\omega\pi \ = \ 0. \tag{53}$$

Similarly, multiplying (52) by x^β and letting $x \rightarrow 0$ we find

$$\frac{\phi_1(0)}{d^\omega}\left\{cot3\pi + \frac{(p+2)}{C_k\,sin\beta\pi} - \frac{2\,(2+p\,p_1)\,e^{i\beta\pi}}{C_k(p_1\ -\ p_2)\,sin\beta\pi\ p_1^\beta}\right.$$
$$\left. + \frac{2\,(2+p\,p_2)\,e^{i\beta\pi}}{C_k(p_1\ -\ p_2)\,sin\beta\pi\ p_2^\beta}\right\} \ = \ 0. \tag{54}$$

Since $\phi_1(0)$ and $\phi_1(d)$ are non-zero, from (53) and (54) we obtain the following characteristic equations to determine ω and β.

$$cot\omega\pi \;=\; 0, \tag{55}$$

$$cot\beta\pi + \frac{(p+2)}{C_h\ sin\beta\pi} - \frac{2\left\{2 + p\ p_1\right\} e^{i\beta\pi}}{C_h(p_1 - p_2)\ sin\beta\pi\ p_1^{\beta}}$$

$$+ \frac{2\left\{2 + p\ p_2\right\} e^{i\beta\pi}}{C_h(p_1 - p_2)\ sin\beta\pi\ p_2^{\beta}} \;=\; 0. \tag{56}$$

From (55) it is seen that $\omega = 1/2$ which is the expected result for the singularity at a crack tip embedded in a homogeneous medium. Equation (56) has to be solved numerically to determine the value of β. From (50) it can be seen that p_1 and p_2 are real for $C_h > 0$ and are complex for $C_h < 0$. This implies that, depending on the sign of C_h, (56) gives two separate characteristic equations. A numerical code was developed to solve (56) for positive and negative values of C_h and it was determined that it does not have a root in the strip $0 < Re(\beta) < 1$. $\beta = 1$ is seen to be a root but is unacceptable [19]. This implies that the unknown function $f_1(t)$ does not have a power singularity at the end point $x = t = 0$.

The next step in the analysis is to check for a weaker, namely for a logarithmic singularity in the unknown function when $c = 0$. From the foregoing analysis we note that for $c = 0$ the solution of the integral equation is of the form

$$f_1(t) \;=\; \frac{\phi(t)}{(d - t)^{\frac{1}{2}}}, \tag{57}$$

thus from (46) and (57) the asymptotic behavior of $F(z)$ near the ends $z = 0$ and $z = d$, respectively, is found to be

$$F(z) \;=\; -\frac{\phi(0)\ log\ z}{\pi\sqrt{d}} + F_1(z), \tag{58}$$

$$F(z) \;=\; \frac{\phi(d)\ log(z - d)}{\pi\sqrt{d}} + F_2(z), \tag{59}$$

where $\phi(t)$, $F_1(z)$ and $F_2(z)$ are bounded functions. By substituting from (57) and (58) into (51) it may be easily shown that the coefficient of the singular term $log\ x$ vanishes. One may, therefore, conclude that at $x = 0$ $f_1(x)$ and, consequently, the stresses are

nonsingular.

We now observe that for $c = 0$ by defining the normalized quantities

$$x = \frac{d}{2}(r+1), \quad t = \frac{d}{2}(u+1), \quad \frac{f_1(t)}{\sigma_o} = \sigma(u), \tag{60}$$

the integral equation (39) may be expressed as

$$\frac{1}{\pi}\int_{-1}^{1}\frac{\sigma(u)}{u-r}\,du + \int_{-1}^{1} N[s(r),\, t(u)]\, f_1(t)\, dt = -1, \ (-1 < r < 1), \tag{61}$$

where $N[s(r),\, t(u)]$ is given by (40) for the orthotropic and (42) for the isotropic half-plane. From (57) it is clear that the solution of (61) is of the form

$$\sigma(u) = w(u)\, G(u), \; w(u) = (1-u)^{-\frac{1}{2}}(1+u)^{0}. \tag{62}$$

One way to solve the problem would be to express the bounded function $G(u)$ in terms of a series of the related orthogonal polynomials, in this case the Jacobi polynomials, as follows:

$$G(u) = \sum_{n=0}^{\infty} A_n\, P_n^{(-\frac{1}{2},\, 0)}(u). \tag{63}$$

Equation (61) may now be reduced to a system of linear algebraic equations in A_n by truncating (63), substituting into (61), and using a collocation technique. The collocation points are chosen according to (36). The following expressions are useful in evaluating the singular integral[20]:

$$\frac{1}{\pi}\int_{-1}^{1}\frac{P_n^{(\alpha,\,\beta)}(t)\,(1-t)^{\alpha}\,(1+t)^{\beta}}{t-s}\,dt = \cot\alpha\pi\,(1-s)^{\alpha}(1+s)^{\beta}P_n^{(\alpha,\,\beta)}(s)$$
$$-\frac{2^{(\alpha+\beta)}\,\Gamma(\alpha)\,\Gamma(n+\beta+1)}{\Gamma(n+\alpha+\beta+1)}\,F\left\{(n+1),\,(-n-\alpha-\beta),\,(1-\alpha),\,\left(\frac{1-s}{2}\right)\right\}, \tag{64}$$

$$\frac{1}{\pi}\int_{-1}^{1}\frac{P_n^{(\alpha,\,\beta)}(t)\,(1-t)^{\alpha}\,(1+t)^{\beta}}{t+u}\,dt = \cot\beta\pi\,(1+u)^{\alpha}(1-u)^{\beta}P_n^{(\beta,\,\alpha)}(u)$$
$$-\frac{2^{(\alpha+\beta)}\,\Gamma(\beta)\,\Gamma(n+\alpha+1)}{\Gamma(n+\alpha+\beta+1)}\,F\left\{(n+1),\,(-n-\alpha-\beta),\,(1-\beta),\,\left(\frac{1-u}{2}\right)\right\}. \tag{65}$$

The hypergeometric function $F(n,\, a,\, b,\, c)$, appearing in (64) and (65), is computed by using the summation formula given in [20]. The integral containing the generalized

Cauchy kernel is evaluated by Gaussian quadrature. The convergence behavior of the numerical scheme is presented in Table 3 which gives the solution for the isotropic half-plane. It is seen from the table that excellent convergence is obtained with an increasing number of terms in the series. For $N = 45$ the value of normalized stress intensity factor matches the exact value computed in [21] upto seven digits beyond the decimal point. The exact value of 1.12152226 was computed in [21] where it was stated that the only possible error might be in the last digit. This technique is used in all edge crack problems in this study.

After determining the unknown function, the stress intensity factor for an edge crack in an orthotropic half-plane may be obtained from (44). For different C_h values, the normalized stress intensity factor is tabulated in Table 4. The results are seen to deviate significantly from the the familiar isotropic result (= 1.1215), when C_h is different from zero. As in the internal crack case, the stress intensity factor is a decreasing function of C_h. Convergence in the numerical solution was observed to be very rapid for positive values of C_h. However, it becomes increasingly difficult to obtain convergent results for $C_h < -1$. The results presented in Table 4 are accurate upto the digits shown. They have been obtained by increasing the number of terms in the series and the quadrature points. Convergence for $C_h < -3.9$ was extremely difficult and the present scheme yields unreliable results. By letting $C_h = -4 + \epsilon$, a singular perturbation technique may be developed to solve the problem. However, the results would be of no practical interest. In the other limiting case, for $C_h \rightarrow \infty$ from (27) it may be shown that the Fredholm kernel becomes

$$N(x, t) = \frac{1}{\pi} \frac{1}{(t + x)} . \tag{66}$$

Thus, by substituting from (66) into (39) and assuming $f_1(t) = -f_1(-t)$, the integral equation may be reduced to

$$\frac{1}{\pi} \int_{-d}^{d} \frac{f_1(t)}{t - x} \, dt = \frac{2 \sigma_o}{K_n} , (-d < x < d), \tag{67}$$

giving

$$f_1(x) = \frac{2 \sigma_o}{K_n} \frac{x}{\sqrt{d^2 - x^2}} . \tag{68}$$

From (44) and (68) it then follows that

$$k_1(d) = \sigma_o \sqrt{d}\,, \tag{69}$$

that is, in Table 4 the normalized stress intensity factor would approach one as C_h goes to infinity.

5. Solution of the Crack Problem for a Single Stiffener

Referring to Fig.1, for $c > 0$, the system of singular integral equations (15)-(17) may be solved by using, for example, the technique described in the previous section in a straightforward manner. The quantities of interest to be calculated are the stress intensity factors which, for the case of a single film shown in Fig.1 may be defined as follows:

$$k_1(c) = \lim_{x \to c} \sqrt{2(c - x)}\, \sigma_{yy}(x, 0)\,, \tag{70}$$

$$k_1(d) = \lim_{x \to d} \sqrt{2(x - d)}\, \sigma_{yy}(x, 0)\,, \tag{71}$$

$$k_2(c) = \lim_{x \to c} \sqrt{2(c - x)}\, \sigma_{xy}(x, 0)\,, \tag{72}$$

$$k_2(d) = \lim_{x \to d} \sqrt{2(x - d)}\, \sigma_{xy}(x, 0)\,, \tag{73}$$

$$k_2(-2a) = \lim_{y \to -2a} \sqrt{2(y + 2a)}\, \sigma_{xy}(y, 0)\,, \tag{74}$$

$$k_2(0) = \lim_{y \to 0} \sqrt{-2y}\, \sigma_{xy}(y, 0). \tag{75}$$

An examination of the kernels N_{ij} given by (18)-(26) would show that, for a fixed crack length $(d - c)$ and the film length $2a$, as the crack distance $(d + c)/2$ goes to infinity, the kernels N_{11}, N_{13}, N_{23}, N_{31} and N_{32} would go to zero and the integral equations would uncouple. Also, since N_{11} and N_{22} are invariant with respect to a 90-degree material rotation, the crack tip stress intensity factors would remain unchanged through such a rotation. However, since N_{33} is explicitly dependent on $\lambda = (C_{11}/C_{22})^{\frac{1}{4}}$, even in the uncoupled case the film end stress intensity factors would be affected by a 90-degree material rotation. In the coupled case all kernels are dependent on λ. Consequently, the crack tip as well as the film end stress intensity factors would be affected by a 90-degree material rotation.

Some sample results showing the normalized stress intensity factors in an orthotropic half-plane stiffened by a single membrane and containing an internal crack

are given in Tables 5-7. In these examples, too, it is assumed that the crack angle θ shown in Fig.1 is zero and the elastic properties of the substrate are given in Table 1. Note that the problem has two dimensionless length parameters, $\{(d - c)/2a\}$ characterizing the relative crack length and $\{(d + c)/2a\}$ giving the relative crack location. Aside from the magnitude of the external load σ_o, the third additional variable in the problem is the relative compliance of the film characterized by

$$\lambda_f = \frac{\beta^1_{22}}{\beta_{22}} \left\{\frac{a}{h}\right\}. \tag{76}$$

Table 5 shows the results for a fixed crack length $\{(d - c)/2a\} = 1$, and Table 6 for a fixed (average) distance $\{(d + c)/2a\} = 1$. From Table 5 it may be seen that as the stiffness of the film decreases, (i.e. as λ_f increases) the primary crack tip stress intensity factors $k_1(c)$ and $k_1(d)$ increase and approach the values given in Table 2 (for which $\lambda_f = \infty$). As the crack distance from the surface increases, $k_2(c)$ and $k_2(d)$ tend to zero and the remaining stress intensity factors approach the uncoupled results given in Table 2 and Fig.3 regardless of the value of the film stiffness λ_f. The rapid increase in $k_2(0)$, the stress intensity factor for the interface shear at the film end $x = 0$, as the crack tip approaches the surface, (i.e. as $c \to 0$ or $\{(d + c)/2a\} \to 1$) is due to the interaction of singular stress fields at the crack tip and the film end. Table 6 shows some sample results for the normalized stress intensity factors for a fixed crack distance $\{(d + c)/2a\} = 1$ and various values of the crack length $\{(d - c)/2a\}$ and film compliance coefficient λ_f. Referring to the integral equation (30) and Fig.3, note that the normalizing stress in the figure is

$$\sigma_o' = \frac{\lambda \sigma_o}{\sqrt{C_h + 4}}, \tag{77}$$

which, for isotropic materials becomes $\sigma_o' = \sigma_o/2$. Therefore, in comparing the results in Tables 5 and 6 with that of Fig.3, the values given in Fig.3 need to be multiplied by a factor of $\{\lambda/\sqrt{C_h + 4}\}$.

The results found in this study for isotropic materials compare well with that of [8] (see also [17]). The slight discrepancy that may exist is due to different techniques used in the respective numerical analyses. The effect of 90-degree material rotation on the stress intensity factors is shown in Table 7. The example is given only for C_h = 6.8222, Material 1A. Except for a 90-degree rotation, the substrate material (Mat.1A) used in Table 7 is the same as that used in Tables 5 and 6 (Mat.1), and in both cases C_h = 6.8222. That is, referring to Table 1, it is assumed that in Tables 5 and 6 C_{11} =

1.0100 x 10^{11}, C_{22} = 0.3592 x 10^{11} and in Table 7 C_{11} = 0.3592 x 10^{11}, C_{22} = 1.0100 x 10^{11} N/m^2, C_{12}, C_{66} and C_h being the same. Note that the stress intensity factors for the material orientation used in Tables 5 and 6 are consistently higher than that given in Table 7 and the differences appear to be significant.

In the important case of an edge crack ($c = 0$, $\theta = 0$, Fig.1) the integral equations (15)-(17) are still valid. However, they now have generalized Cauchy kernels which become unbounded as x, t, y, y_o approach the end point $x = 0$, $y = 0$ simultaneously. Unlike the edge crack problem in the absence of a stiffner, described in the previous section, in this case it is not possible to make an intuitive statement about the nature of the singularity at the common end points of the crack and the film. This singularity may be examined in a straightforward manner by defining

$$\frac{K_n}{2} f_1(t) = \frac{\phi_1(t)}{t^\beta (d - t)^\omega}, (0 < Re(\beta, \omega) < 1) \tag{78}$$

$$\frac{K_e}{2} f_2(t) = \frac{\phi_2(t)}{t^\beta (d - t)^\gamma}, (0 < Re(\beta, \gamma) < 1) \tag{79}$$

$$f_3(y_o) = \frac{\phi_3(y_o)}{(-y_o)^\beta (y_o + 2a)^\alpha}, (0 < Re(\beta, \alpha) < 1) \tag{80}$$

and by following a function-theoretic mathod briefly described in the previous section. For the remote singular points the characteristic equations are found to be

$$cot\omega\pi = 0, cot\gamma\pi = 0, cot\alpha\pi = 0. \tag{81}$$

giving $\omega = \gamma = \alpha = 1/2$. The characteristic equation found for the endpoint $x = 0 = y$ is rather complicated[17]. However, its examination shows that it has no root in the complex strip $0 < \mathrm{Re}(\beta) < 1$. Thus the unknown functions f_1, f_2 and f_3 have no power singularity at $x = y = 0$ and, hence, may be expressed as

$$\frac{K_n}{2} f_1(t) = \frac{G_1(t)}{\sqrt{d - t}}, \quad \frac{K_e}{2} f_2(t) = \frac{G_2(t)}{\sqrt{d - t}}, \quad f_3(y_o) = \frac{G_3(y_o)}{\sqrt{y_o + 2a}}, \tag{82}$$

where G_i, (i = 1, 2, 3) are bounded functions and are nonzero at the end points. Searching now for a logarithmic singularity at the point $x = y = 0$, after performing the appropriate asymptotic analysis from (15)-(17) and (82) it can be shown that the coefficients of the logarithmic terms cancel out and

$$- G_3(0) \log -y < \infty, \mathrm{y} \leq 0, \tag{83}$$

giving $G_3(0) = 0$. This would imply that the apex of the 90-degree wedge formed by the intersection of the crack and the membrane is stress free.

In the case of a single stiffener and an edge crack (Fig.1, $c = 0$, $\theta = 0$), after normalizing the intervals, from (82) it may be shown that for f_1 and f_2 the weight function and the related orthogonal polynomial are $(1 - t)^{-\frac{1}{2}}(1 + t)^0$ and $P_n^{(-\frac{1}{2}, 0)}(t)$ and for f_3 $(1 - t)^0 (1 + t)^{-\frac{1}{2}}$ and $P_n^{(0, -\frac{1}{2})}(t)$, respectively. The technique to solve the integral equations would then be quite similar to that described in the previous section. Note that in this edge crack problem the equilibrium condition (13) is the only external condition that needs to be satisfied in solving the integral equations.

After solving the integral equations the stress intensity factors are determined from (71), (73) and (74). Some sample results obtained for $C_h = 6.8222$, 3.0358, -1.0944 and -1.3137 corresponding to materials 1, 2, 5 and 6, respectively (see Table 1), are shown in Table 8 for various stiffness ratios λ_f and relative dimensions d/a. Physically it is expected that as $(d/a) \to \infty$ (for all values of λ_f) and as $\lambda_f \to \infty$ (for all values of (d/a)), $k_2(d)$ would approach zero and k_1(d) would tend to the edge crack results for an unstiffened orthotropic half-plane given in Table 4. This trend may indeed be observed in Table 8. Similarly, as $(d/a) \to 0$ the stress intensity factor for the interface shear, $k_2(-2a)$ would be expected to approach the results given in Fig.3. This, too, may be seen in Table 8 again with the understanding that to conform to the notation given in Fig.3, the results given in Table 8 must be multiplied by $\sqrt{(C_h + 4)}/\lambda$. Note that the interaction between the membrane stiffener and the crack is much stronger in the edge crack case than it is for the internal crack problem. The table shows that generally all stress intensity factors decrease with both increasing C_h and increasing compliance constant λ_f. One of the more significant results of the edge crack problem is, of course, the fact that the interface shear stress intensity factor $k_2(0)$ at the film end $x = 0$ is zero. The effect of a 90-degree material rotation on the stress intensity factors is shown in Table 9. The results given in Table 8 are based on the material constants shown in Table 1. In Table 9 the 90-degree rotation is accomplished simply by interchanging C_{11} and C_{22} in the substrate. In this case, too, the stress intensity factors for the material orientation corresponding to Table 8 are seen to be consistently greater than that given in Table 9. Not unexpectedly, the differences between the two sets of results are seen to be much more pronounced for small values of (d/a).

Some sample results for the distribution of the interface shear stress in an isotropic half-plane containing a crack and stiffened by a single membrane are also given

in Fig.5. Curve 1 shows the result for the edge crack case $c = 0$. Note that in this particular case at the endpoint $y = 0$, the interface shear stress is zero. For reference, the figure also shows the shear stress for $c = \infty$ (curve 4) corresponding to the uncoupled problem. Also note that as the ligament size c decreases, there is a considerable increase in the interface shear near $y = 0$.

6. The Broken Film on a Cracked Substrate

The problem is described in Fig.2. In this case by observing that $f_2(t) = 0$ and by using the symmetry conditions, the integral equations (15)-(17) may be expressed as

$$\frac{1}{\pi}\int_0^d \frac{f_1(t)}{t-x}\,dt + \int_0^d Q_{11}(x,\,t)\,f_1(t)\,dt + \int_{-2a}^0 Q_{13}(x,\,y_o)\,f_3(y_o)\,dy_o = g_1(x),\ (0 < x < d), \tag{84}$$

$$\frac{1}{\pi}\int_{-2a}^0 \frac{f_3(y_o)}{y_o - y}\,dy_o + \int_0^d Q_{21}(y,\,t)\,f_1(t)\,dt + \int_{-2a}^0 Q_{23}(y,\,y_o)\,f_3(y_o)\,dy_o = g_2(y),\ (-2a < y < 0), \tag{85}$$

where

$$Q_{11}(x,\,t) = \frac{2}{\pi\,C_h}\left\{\frac{(C_h+4)}{2\,(x+t)} - \frac{\{2\,x + t\,(C_h+2)\}}{\left\{x^2 + (C_h+2)\,x\,t + t^2\right\}}\right\}, \tag{86}$$

$$Q_{13}(x,\,y_o) = \frac{4\,\sqrt{(C_h+4)}\,y_o^3\,\lambda^3}{\pi\,K_n\left\{(y_o^2 + \lambda^2\,x^2)^2 + C_h\,x^2\lambda^2 y_o^2\right\}}, \tag{87}$$

$$Q_{21}(y,\,t) = -\frac{K_n(C_h+4)\,t\,\lambda^3 y^2}{\pi\left\{(t^2 + \lambda^2\,y^2)^2 + C_h\,y^2\lambda^2 t^2\right\}\sqrt{(C_h+4)}}, \tag{88}$$

$$Q_{23}(y,\,y_o) = \frac{1}{\pi\,(y_o + y)} - \frac{\beta_{22}^1\ \lambda\,H\,(y - y_o)}{\beta_{22}\ h\,\sqrt{(C_h+4)}}, \tag{89}$$

$$g_1(x) = \frac{2\,\sigma_o}{K_n},\quad g_2(y) = \frac{\lambda\,\sigma_o}{\sqrt{(C_h+4)}}. \tag{90}$$

In this case too, the asymptotic analysis shows that at the end point $x = y = 0$ the functions f_1 and f_3 are bounded and have the form as given by (82) (see [17]). The

solution may, therefore, be obtained by normalizing the intervals and by expressing G_1 and G_2 in terms of series of Jacobi polynomials.

Some sample results for normalized stress intensity factors are listed in Table 10. Table 11 shows the effect of the 90-degree material rotation. Comparing the results given in Tables 8 and 9 with those of Tables 10 and 11, it may be seen that the stress intensity factors for the case of two symmetric membranes are consistently greater than the single membrane case. It may also be observed that, in general, the stress intensity factors increase with decreasing C_h.

7. Conclusions

The membrane model used in this paper for thin film overlays on elastic substrates appears to be a good first approximation to various stress concentration problems in the composite medium. The results obtained in the form of stress intensity factors may be useful in the study of such mechanical failure problems as film debonding, film rupture and substrate cracking. The analysis was carried out for orthotropic films and orthotropic substrates. The results found indicate that the material orthotropy may have a significant influence on the stress intensity factors at the crack tips and along the film edges. One major limitation of the model is neglecting the bending stiffness of the film. As a consequence of this the normal component of the stress along the interface is assumed to be zero, which is not realistic. Since the elastic continuum model for thin films leads to rather insurmountable analytical and computational difficulties, a "plate" model appears to be the obvious compromise. The crack problem for an orthotropic half-plane stiffened by a plate will be the topic of our next paper on the subject.

Acknowledgements: This research was supported by the National Science Foundation under Grant MSS-8917867 and by the Office of Naval Research Contract N00014-89-33188.

REFERENCES

[1] Hu, S. M., "Film-Edge-Induced Stress in Substrates," *Journal of Applied Physics*, **50 (7)** (1979), pp. 4661-4666.

[2] Isomae, S., "Stress in Silicon at Si_3N_4/SiO_2 Film Edges and Viscoelastic Behavior of SiO_2 Films," *Journal of Applied Physics*, **57 (2)** (1985), pp. 216-223.

[3] Isomae, S., "Stress Distributions in Silicon Crystal Substrates with Thin Films," *Journal of Applied Physics*, **52 (4)** (1981), pp. 2782-2791.

[4] Arutiunian, N. Kh., "Contact Problem for a Half-Plane with Elastic Reinforcement," *Journal of Applied Mathematics and Mechanics (PMM)*, **32 (4)** (1968), pp. 652-665.

[5] Arutiunian, N. Kh. and Mikhitarian, S. M., "Periodic Contact Problem for a Half-Plane with Elastic Laps (Cover Plates)," *Journal of Applied Mathematics and Mechanics (PMM)*, **33 (5)** (1969), pp. 813-843.

[6] Erdogan, F., "Analysis of Elastic Cover Plates," *Developments in Mechanics, Proceedings of the 12th Midwestern Mechanics Conference*, **6** (1971), pp. 817-830.

[7] Erdogan, F. and Gupta, G. D., "The Problem of an Elastic Stiffener Bonded to a Half-Plane," *Journal of Applied Mechanics*, **38**, *Transactions of the ASME* (1971), pp. 937-942.

[8] Delale, F. and Erdogan, F., "The Crack Problem for a Half-Plane Stiffened by Elastic Cover Plates," *International Journal of Solids and Structures*, **18 (5)** (1982), pp. 381-395.

[9] Erdogan, F. and Joseph, P. F., "Mechanical Modelling of Multilayered Films on an Elastic Substrate - Parts I and II," *Journal of Electronic Packaging*, **112** *Transactions of the ASME* (1990), pp. 309-326.

[10] Goodier, J. N. and Hsu, C. S., "Transmission of Tension from a Bar to a Plate," *Journal of Applied Mechanics*, **21**, *Transactions of the ASME*, (1954), pp. 147-150.

[11] Erdogan, F. and Civelek, M. B., "Contact Problem for an Elastic Reinforcement Bonded to an Elastic Plate," *Journal of Applied Mechanics*, **41**, *Transactions of the ASME*, (1974), pp. 1014-1018.

[12] Pande, C. S. and Chou, Y. T., "Edge Dislocations in Semi-Infinite Anisotropic Media," *physica status solidi*, Series a **(6)** (1971), pp. 499-504.

[13] Wu, R. S. and Chou, Y. T., "Line Force in a Two-Phase Orthotropic Medium," *Journal of Applied Mechanics*, **49** *Transactions of the ASME*, (1982), pp. 55-61.

[14] Chou, Y. T., "Interaction of Parallel Dislocations in a Hexagonal Crystal," *Journal of Applied Physics*, **33 (9)** (1962), pp. 2747-2751.

[15] Cinar, A. and Erdogan, F., "The Crack and Wedging Problem for an Orthotropic Strip," *International Journal of Fracture*, **23** (1983), pp. 83-102.

[16] Krenk, S., "On the Elastic Constants of Plane Orthotropic Elasticity," *Journal of Composite Materials*, **13** (1979), pp. 108-116.

[17] Mahajan, R. V., "Contact and Crack Problems for an Orthotropic Half-Plane Stiffened by Elastic Films," *Phd Dissertation*, Lehigh University (1992).

[18] Delale, F. and Erdogan, F., "The Problem of Internal and Edge Cracks in an Orthotropic Strip," *Journal of Applied Mechanics*, **44** *Transactions of the ASME*, (1977), pp. 237-242.

[19] Erdogan, F., "Mixed Boundary-Value Problems in Mechanics," *Mechanics Today*, Vol. IV S. Nemat-Nasser (ed.) Pergamon Press, Oxford (1978), pp. 1-86.

[20] Abramovitz, M. and Stegun, I. A., "Handbook of Mathematical Functions," Dover Publications, Inc., New York, (1965).

[21] Kaya, A. C., "Applications of Integral Equations with Strong Singularities in Fracture Mechanics," *Phd Dissertation*, Lehigh University (1984).

Appendix A
Green's Functions for Stresses in an Orthotropic Half-Plane

Consider an orthotropic elastic solid having the constitutive relations

$$\begin{bmatrix} \sigma_{11} \\ \sigma_{22} \\ \sigma_{33} \\ \sigma_{23} \\ \sigma_{13} \\ \sigma_{12} \end{bmatrix} = \begin{bmatrix} C_{11} & C_{12} & C_{13} & 0 & 0 & 0 \\ C_{12} & C_{22} & C_{23} & 0 & 0 & 0 \\ C_{13} & C_{23} & C_{33} & 0 & 0 & 0 \\ 0 & 0 & 0 & C_{44} & 0 & 0 \\ 0 & 0 & 0 & 0 & C_{55} & 0 \\ 0 & 0 & 0 & 0 & 0 & C_{66} \end{bmatrix} \begin{bmatrix} \epsilon_{11} \\ \epsilon_{22} \\ \epsilon_{33} \\ \gamma_{23} \\ \gamma_{13} \\ \gamma_{12} \end{bmatrix} \tag{A1}$$

where $\left[\; C_{ij} \; \right]$ is the stiffness matrix. The Green's functions due to a pair of dislocations at a point (x_1, y_1) in the half-plane, appearing in (1) are found to be [12]

$$\begin{aligned} & K_{11}(x, y, x_1, y_1) \; = \\ & \frac{K_n \lambda^2}{2\pi} \left\{ \frac{(x - x_1)}{\chi_1} \left\{ (x - x_1)^2 - \lambda^2 (y - y_1)^2 \right\} \right. \\ & \left. - \frac{(x + x_1)}{\chi_2} \left\{ (x + x_1)^2 - \lambda^2 (y - y_1)^2 \right\} \right\} \\ & + \frac{K_n \lambda^2}{\pi C_h} \left\{ \frac{(x + x_1)}{\chi_2} \left\{ 2\zeta + C_h (x + x_1)^2 \right\} - \frac{1}{\chi_3} \{ 2 (x + x_1) \zeta \right. \\ & \left. + C_h \left\{ C_h x_1 x^2 + x (x + x_1) (x + 3 x_1) + x_1 \lambda^2 (y - y_1)^2 \right\} \right\} \right\}, \end{aligned} \tag{A2}$$

$$\begin{aligned} & K_{12}(x, y, x_1, y_1) \; = \\ & - \frac{K_e \lambda^2}{2\pi} \left\{ \frac{(y - y_1)}{\chi_1} \left\{ (C_h + 3) (x - x_1)^2 + \lambda^2 (y - y_1)^2 \right\} \right. \\ & \left. - \frac{(y - y_1)}{\chi_2} \left\{ (C_h + 3) (x + x_1)^2 + \lambda^2 (y - y_1)^2 \right\} \right\} \\ & + \frac{K_e \lambda^2}{\pi C_h} \left\{ \frac{(y - y_1)}{\chi_2} \left\{ 2\zeta + C_h (x + x_1)^2 \right\} \right. \end{aligned}$$

$$- \frac{(y - y_1)}{\chi_3} \left\{ 2\,\zeta + C_h(x^2 + x_1^2) \right\} \Bigg\}, \tag{A3}$$

$$K_{21}\,(x,\, y,\, x_1,\, y_1) \;=$$

$$\frac{K_n\,\lambda^2}{2\,\pi} \Bigg\{ \frac{(y - y_1)}{\chi_1} \left\{ (x - x_1)^2 - \lambda^2\,(y - y_1)^2 \right\}$$

$$- \frac{(y - y_1)}{\chi_2} \left\{ (x + x_1)^2 - \lambda^2\,(y - y_1)^2 \right\} \Bigg\}$$

$$+ \frac{K_n\,\lambda^2}{\pi\,C_h} \Bigg\{ \frac{(y - y_1)}{\chi_2} \left\{ 2\,\zeta + C_h\,(x + x_1)^2 \right\}$$

$$- \frac{(y - y_1)}{\chi_3} \left\{ 2\,\zeta + C_h(x^2 + x_1^2) \right\} \Bigg\}, \tag{A4}$$

$$K_{22}\,(x,\, y,\, x_1,\, y_1) \;=$$

$$\frac{K_e}{2\,\pi} \Bigg\{ \frac{(x - x_1)}{\chi_1} \left\{ (x - x_1)^2 - \lambda^2\,(y - y_1)^2 \right\}$$

$$- \frac{(x + x_1)}{\chi_2} \left\{ (x + x_1)^2 - \lambda^2\,(y - y_1)^2 \right\} \Bigg\}$$

$$- \frac{K_e}{\pi\,C_h} \Bigg\{ \frac{(x + x_1)}{\chi_2} \left\{ 2\,\zeta + C_h\,\lambda^2\,(y - y_1)^2 \right\} - \frac{1}{\chi_3} \{ 2\,(x + x_1)\,\zeta$$

$$+ C_h \Big\{ C_h\,x\,x_1^2 + x_1\,(x + x_1)\,(3\,x + x_1) + x\,\lambda^2 (y - y_1)^2 \Big\} \Bigg\} \Bigg\}, \tag{A5}$$

$$K_{31}\,(x,\, y,\, x_1,\, \mathrm{y}_1) \;=$$

$$\frac{K_n}{2\,\pi} \Bigg\{ \frac{(x - x_1)}{\chi_1} \left\{ (x - x_1)^2 + (C_h + 3)\,\lambda^2\,(y - y_1)^2 \right\}$$

$$- \frac{(x + x_1)}{\chi_2} \left\{ (x + x_1)^2 + (C_h + 3)\,\lambda^2\,(y - y_1)^2 \right\} \Bigg\}$$

$$- \frac{K_n}{\pi\,C_h} \Bigg\{ \frac{(x + x_1)}{\chi_2} \left\{ 2\,\zeta + C_h\,\lambda^2\,(y - y_1)^2 \right\} - \frac{1}{\chi_3} \{ 2\,(x + x_1)\,\zeta$$

$$+ C_h \Big\{ C_h\,x\,x_1^2 + x_1\,(x + x_1)\,(3\,x + x_1) + x\,\lambda^2 (y - y_1)^2 \Big\} \Bigg\} \Bigg\}, \tag{A6}$$

$$K_{32}\,(x,\, y,\, x_1,\, y_1) \;=$$

$$\frac{K_e}{2\,\pi}\left\{\frac{(y\,-\,y_1)}{\chi_1}\left\{(x\,-\,x_1)^2\,-\,\lambda^2\,(y\,-\,y_1)^2\right\}\right.$$

$$\left.-\,\frac{(y\,-\,y_1)}{\chi_2}\left\{(x+x_1)^2\,-\,\lambda^2\,(y\,-\,y_1)^2\right\}\right\}$$

$$-\,\frac{K_e}{\pi\,C_h}\left\{\frac{(y\,-\,y_1)}{\chi_2}\left\{2\,\zeta\,+\,C_h\,\lambda^2(y\,-\,y_1)^2\right\}\,-\,\frac{(y\,-\,y_1)}{\chi_3}\{2\,\zeta\right.$$

$$\left.+\,C_h\left\{(C_h+4)\,x_1^2+2\,x_1x+\lambda^2\,(y\,-\,y_1^2)\right\}\right\}\right\}, \tag{A7}$$

where

$$\lambda\;=\;\left\{\frac{C_{11}}{C_{22}}\right\}^{\frac{1}{4}}, \tag{A8}$$

$$K_e=(\overline{C}_{12}+C_{12})\left\{\frac{C_{66}\,(\overline{C}_{12}\,-\,C_{12})}{C_{22}\,(\overline{C}_{12}+C_{12}+2\,C_{66})}\right\}^{\frac{1}{2}}, \tag{A9}$$

$$\overline{C}_{12}=\{C_{11}\;C_{22}\}^{\frac{1}{2}}, \tag{A10}$$

$$K_n\;=\frac{K_e}{\lambda^2}\,, \tag{A11}$$

$$C_h=\frac{(\overline{C}_{12}+C_{12})\,(\overline{C}_{12}\,-\,C_{12}\,-\,2\,C_{66})}{\overline{C}_{12}\,C_{66}}\,, \tag{A12}$$

$$\zeta\;\;=\;(x+x_1)^2+\lambda^2\,(y\,-\,y_1)^2, \tag{A13}$$

$$\chi_1\;=\;\left\{(x\,-\,x_1)^2+\lambda^2\,(y\,-\,y_1)^2\right\}^2+C_h\,(x\,-\,x_1)^2\,\lambda^2\,(y\,-\,y_1)^2, \tag{A14}$$

$$\chi_2\;=\;\zeta^2+C_h\,(x+x_1)^2\,\lambda^2\,(y\,-\,y_1)^2, \tag{A15}$$

$$\chi_3\;=\;(\zeta+C_h\,x_1x)^2+C_h\,(x\,-\,x_1)^2\,\lambda^2\,(y\,-\,y_1)^2. \tag{A16}$$

Similarly the Green's functions for a pair of concentrated forces acting at a point $(0,\,y_o)$ on the boundary are given by [13]

$$K_{13}(x,\,y,\,y_o)\;\;=$$

$$-\,\frac{\lambda^3\,x^2(y\,-\,y_o)\,\sqrt{(C_h+4)}}{\pi\left\{x^4+\lambda^2\,(C_h+2)\,x^2\,(y\,-\,y_o)^2+\lambda^4\,(y\,-\,y_o)^4\right\}}\,, \tag{A17}$$

$$K_{14}(x,\ y,\ y_o) \quad =$$

$$-\ \frac{\lambda\ x^3\ \sqrt{(C_h+4)}}{\pi\left\{x^4+\lambda^2\ (C_h+2)\ x^2\ (y\ -\ y_o)^2+\lambda^4\ (y\ -\ y_o)^4\right\}}, \tag{A18}$$

$$K_{23}(x,\ y,\ y_o) \quad =$$

$$-\ \frac{\lambda^3\ x\ (y\ -\ y_o)^2\ \sqrt{(C_h+4)}}{\pi\left\{x^4+\lambda^2\ (C_h+2)\ x^2\ (y\ -\ y_o)^2+\lambda^4\ (y\ -\ y_o)^4\right\}}, \tag{A19}$$

$$K_{24}(x,\ y,\ y_o) \quad =$$

$$-\ \frac{\lambda\ x^2\ (y\ -\ y_o)\ \sqrt{(C_h+4)}}{\pi\left\{x^4+\lambda^2\ (C_h+2)\ x^2\ (y\ -\ y_o)^2+\lambda^4\ (y\ -\ y_o)^4\right\}}, \tag{A20}$$

$$K_{33}(x,\ y,\ y_o) \quad =$$

$$-\ \frac{\lambda^3\ (y\ -\ y_o)^3\ \sqrt{(C_h+4)}}{\pi\left\{x^4+\lambda^2\ (C_h+2)\ x^2\ (y\ -\ y_o)^2+\lambda^4\ (y\ -\ y_o)^4\right\}}, \tag{A21}$$

$$K_{34}(x,\ y,\ y_o) \quad =$$

$$-\ \frac{\lambda\ x\ (y\ -\ y_o)^2\ \sqrt{(C_h+4)}}{\pi\left\{x^4+\lambda^2\ (C_h+2)\ x^2\ (y\ -\ y_o)^2+\lambda^4\ (y\ -\ y_o)^4\right\}}. \tag{A22}$$

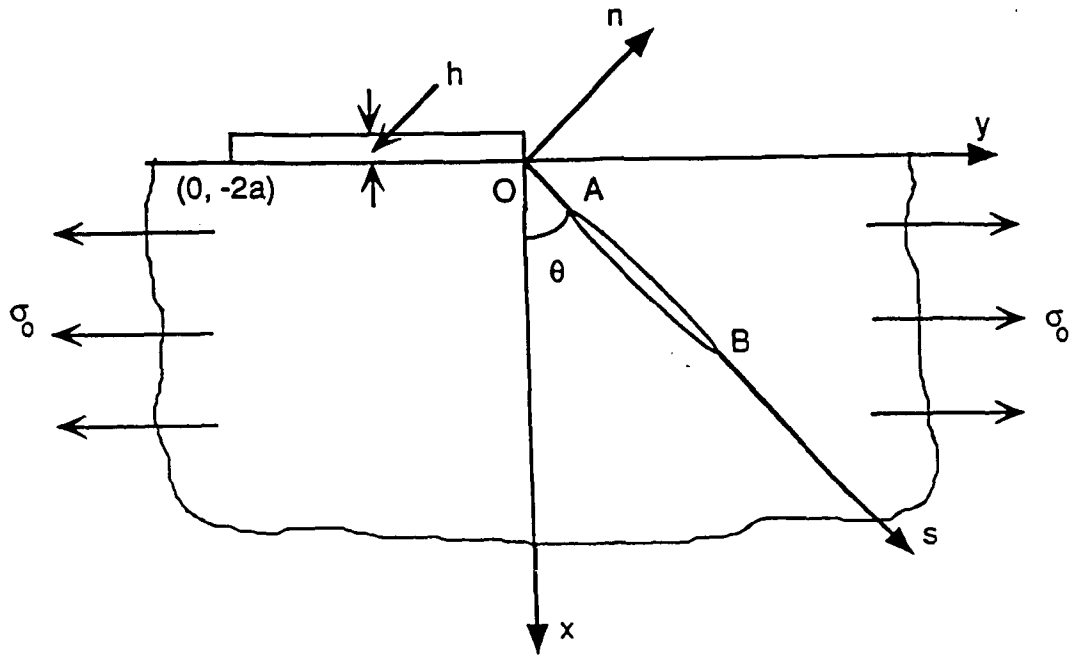

Fig.1. Schematic diagram illustrating the loading and geometry for the problem of an internally cracked half-plane stiffened by a film.

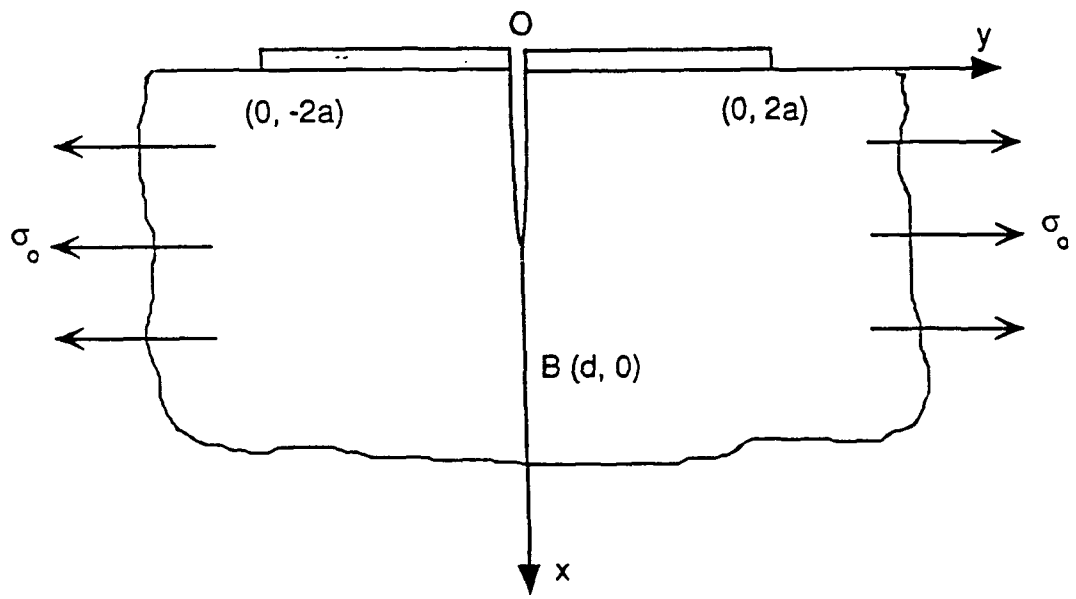

Fig.2. Schematic diagram illustrating the loading and geometry for the problem of an edge cracked half-plane stiffened by symmetric film.

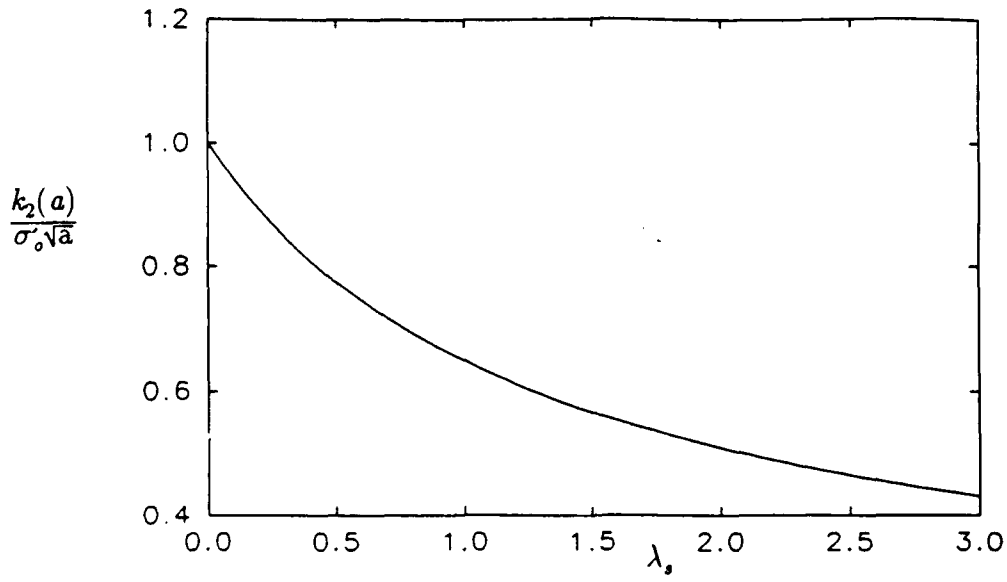

Fig.3. Variation of the normalized film edge stress intensity factor with stiffness parameter λ_s

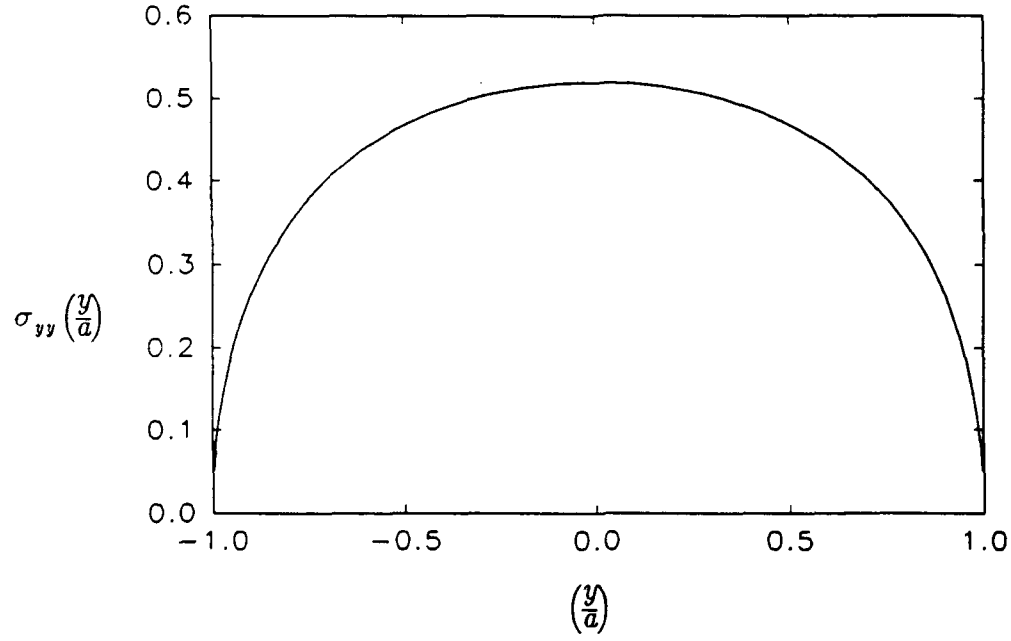

Fig.4. Typical variation of the normalized film stress along the contact region.

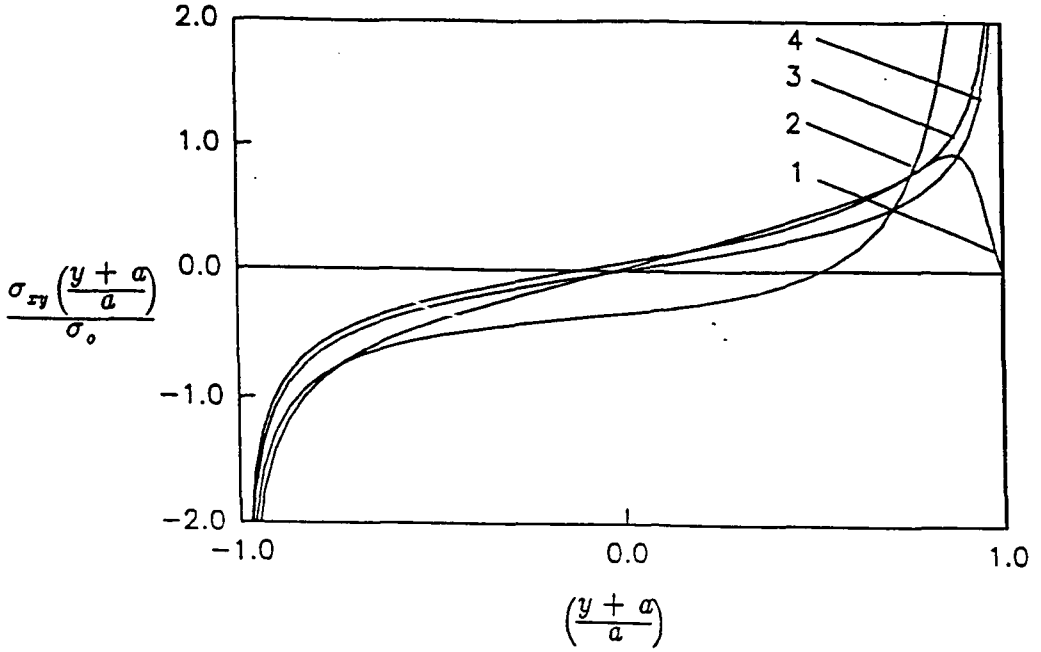

Fig.5. Interface shear distribution for an isotropic half-plane containing a crack and stiffened by a single membrane (Fig. 1, $\theta = 0$); the curves 1 through 4 correspond to $c/a = 0$ (the edge crack), 0.1, 1.0 and ∞.

Material	C_{11} $\times 10^{11} \frac{N}{m^2}$	C_{12} $\times 10^{10} \frac{N}{m^2}$	C_{22} $\times 10^{11} \frac{N}{m^2}$	C_{66} $\times 10^{10} \frac{N}{m^2}$	C_h
1	1.0100	2.7430	0.3592	0.4905	6.8222
2	0.5966	0.6764	0.1712	0.5592	3.0358
3	0.2097	0.8989	0.2097	0.5993	0.0000
4	0.2088	0.9012	0.2101	0.5971	-0.0022
5	1.6800	6.6000	1.6800	8.4000	-1.0944
6	1.1904	5.3840	1.1904	5.9520	-1.3137

Table 1. Stiffness coefficients C_{ij} for the orthotropic half-planes used in the examples.

C_h	6.8222		3.0358		0.0000	
$\frac{d+c}{d-c}$	$\frac{k_1(c)}{k_o}$	$\frac{k_1(d)}{k_o}$	$\frac{k_1(c)}{k_o}$	$\frac{k_1(d)}{k_o}$	$\frac{k_1(c)}{k_o}$	$\frac{k_1(d)}{k_o}$
1.02	2.6753	1.2436	2.7540	1.2646	2.8820	1.3009
1.04	2.1411	1.2127	2.2048	1.2321	2.3081	1.2661
1.06	1.8925	1.1922	1.9485	1.2106	2.0394	1.2430
1.08	1.7402	1.1768	1.7910	1.1943	1.8740	1.2253
1.10	1.6348	1.1643	1.6816	1.1810	1.7584	1.2108
1.12	1.5563	1.1537	1.5999	1.1698	1.6719	1.1985
1.14	1.4952	1.1447	1.5360	1.1602	1.6040	1.1879
1.16	1.4459	1.1367	1.4849	1.1517	1.5487	1.1786
1.18	1.4052	1.1298	1.4415	1.1441	1.5027	1.1703
1.20	1.3709	1.1234	1.4053	1.1373	1.4637	1.1626
1.24	1.3164	1.1126	1.3473	1.1254	1.4008	1.1493
1.28	1.2794	1.1034	1.3028	1.1155	1.3521	1.1382
1.32	1.2418	1.0954	1.2677	1.1069	1.3131	1.1284
1.36	1.2152	1.0887	1.2387	1.0994	1.2811	1.1199
1.40	1.1932	1.0827	1.2148	1.0929	1.2544	1.1123
1.50	1.1520	1.0706	1.1799	1.0793	1.2035	1.0967
1.60	1.1236	1.0611	1.1387	1.0690	1.1676	1.0844
1.80	1.0872	1.0475	1.0984	1.0537	1.1203	1.0664
2.00	1.0653	1.0382	1.0740	1.0434	1.0913	1.0539
$\rightarrow\infty$	1.0000	1.0000	1.0000	1.0000	1.0000	1.0000

Table 2. Normalized stress intensity factors in an orthotropic half-plane with an internal crack, Fig.4, $\theta = 0$, $k_o = \sigma_o\sqrt{(d-c)/2}$, Materials 1-3.

$\frac{k_1(d)}{\sigma_o\sqrt{d}}$	N
1.121518230454	10
1.121522319145	15
1.121522334904	20
1.121522287226	25
1.121522267425	30
1.121522259954	35
1.121522255943	45

Table 3. Convergence of the calculated stress intensity factor for an edge crack in an isotropic half-plane under tension.

C_h	$\frac{k_1(d)}{\sigma_o\sqrt{d}}$
$\rightarrow\infty$	1.0000
10.0	1.0556
9.00	1.0584
8.00	1.0615
7.00	1.0650
6.00	1.0692
5.00	1.0740
4.00	1.0797
3.00	1.0866
2.00	1.0952
1.00	1.1064
0.00	1.1215
-1.00	1.1436
-2.00	1.1803
-3.00	1.2605
-3.40	1.3360
-3.60	1.4074
-3.80	1.5563
-3.90	1.7442

Table 4. The normalized stress intensity factor as a function of C_h for an orthotropic half-plane containing an edge crack under far-field tension.

$\frac{d+c}{2a}$	$\frac{k_1(d)}{\sigma_o\sqrt{\frac{d-c}{2}}}$	$\frac{k_1(c)}{\sigma_o\sqrt{\frac{d-c}{2}}}$	$\frac{k_2(d)}{\sigma_o\sqrt{\frac{d-c}{2}}}$	$\frac{k_2(c)}{\sigma_o\sqrt{\frac{d-c}{2}}}$	$\frac{k_2(0)}{\sigma_o\sqrt{a}}$	$\frac{k_2(-2a)}{\sigma_o\sqrt{a}}$
$\lambda_f = 0.00$						
1.1	1.0778	1.4322	0.0454	-0.0965	0.9847	-0.4760
1.5	1.0288	1.0416	0.0309	0.0184	0.5718	-0.5219
2.0	1.0170	1.0132	0.0223	0.0269	0.4758	-0.4946
3.0	1.0089	1.0073	0.0136	0.0188	0.4222	-0.4466
5.0	1.0040	1.0038	0.0065	0.0088	0.4006	-0.4123
$\lambda_f = 0.20$						
1.1	1.0823	1.4367	0.0438	-0.0882	0.9495	-0.4488
1.5	1.0313	1.0481	0.0291	0.0178	0.5440	-0.4955
2.0	1.0183	1.0165	0.0209	0.0253	0.4521	-0.4708
3.0	1.0094	1.0084	0.0127	0.0176	0.4016	-0.4256
5.0	1.0042	1.0041	0.0061	0.0083	0.3816	-0.3930
$\lambda_f = 1.00$						
1.1	1.0961	1.4521	0.0386	-0.0634	0.8382	-0.3678
1.5	1.0390	1.0679	0.0238	0.0158	0.4592	-0.4157
2.0	1.0223	1.0263	0.0168	0.0205	0.3803	-0.3989
3.0	1.0110	1.0116	0.0101	0.0141	0.3394	-0.3621
5.0	1.0046	1.0048	0.0048	0.0066	0.3239	-0.3346

Table 5. Stress intensity factors in an orthotropic half-plane stiffened by a single membrane and containing an internal crack; Fig.1, $\theta = 0$, $\{(d - c)/2a\} = 1$, $\lambda_f = (\beta^1_{22}/\beta_{22})(a/h)$, Material 1, $C_h = 6.8222$.

$\frac{d-c}{2a}$	$\frac{k_1(d)}{\sigma_o\sqrt{\frac{d-c}{2}}}$	$\frac{k_1(c)}{\sigma_o\sqrt{\frac{d-c}{2}}}$	$\frac{k_2(d)}{\sigma_o\sqrt{\frac{d-c}{2}}}$	$\frac{k_2(c)}{\sigma_o\sqrt{\frac{d-c}{2}}}$	$\frac{k_2(0)}{\sigma_o\sqrt{a}}$	$\frac{k_2(-2a)}{\sigma_o\sqrt{a}}$
$\lambda_f = 0.00$						
0.10	0.9465	0.9401	0.0193	0.0172	0.3962	-0.3952
0.25	0.9560	0.9417	0.0210	0.0151	0.4099	-0.4033
0.50	0.9806	0.9677	0.0253	0.0070	0.4684	-0.4293
0.75	1.0212	1.0859	0.0336	0.0235	0.6257	-0.4582
0.90	1.0685	1.3993	0.0431	-0.0997	0.9256	-0.4536
$\lambda_f = 0.20$						
0.10	0.9500	0.9440	0.0182	0.0163	0.3775	-0.3766
0.25	0.9594	0.9461	0.0198	0.0144	0.3905	-0.3841
0.50	0.9842	0.9736	0.0240	0.0071	0.4463	-0.4081
0.75	1.0254	1.0930	0.0320	-0.0207	0.5983	-0.4339
0.90	1.0731	1.4033	0.0417	-0.0913	0.8923	-0.4280
$\lambda_f = 1.00$						
0.10	0.9604	0.9556	0.0149	0.0135	0.3210	-0.3202
0.25	0.9695	0.9594	0.0162	0.0122	0.3318	-0.3260
0.50	0.9948	0.9912	0.0198	0.0071	0.3791	-0.3442
0.75	1.0381	1.1151	0.0273	-0.0128	0.5134	-0.3611
0.90	1.0874	1.4171	0.0371	-0.0663	0.7874	-0.3514

Table 6. Stress intensity factors in an orthotropic half-plane stiffened by a single membrane and containing an internal crack; Fig.1, $\theta = 0$, $\{(d + c)/2a\} = 1$, $\lambda_f = (\beta^1_{22}/\beta_{22})(a/h)$, Material 1, $C_h = 6.8222$.

$\frac{d+c}{2a}$	$\frac{k_1(d)}{\sigma_\circ\sqrt{\frac{d-c}{2}}}$	$\frac{k_1(c)}{\sigma_\circ\sqrt{\frac{d-c}{2}}}$	$\frac{k_2(d)}{\sigma_\circ\sqrt{\frac{d-c}{2}}}$	$\frac{k_2(c)}{\sigma_\circ\sqrt{\frac{d-c}{2}}}$	$\frac{k_2(0)}{\sigma_\circ\sqrt{a}}$	$\frac{k_2(-2a)}{\sigma_\circ\sqrt{a}}$
$\lambda_f = 0.00$						
1.1	1.1041	1.3985	0.0276	-0.0174	0.6571	-0.4018
1.5	1.0515	1.0817	0.0139	0.0196	0.3452	-0.3744
2.0	1.0307	1.0424	0.0080	0.0136	0.2789	-0.3161
3.0	1.0148	1.0186	0.0039	0.0065	0.2476	-0.2678
5.0	1.0058	1.0068	0.0014	0.0022	0.2372	-0.2435
$\lambda_f = 0.20$						
1.1	1.1062	1.4043	0.0268	-0.0159	0.6409	-0.3880
1.5	1.0522	1.0843	0.0134	0.0189	0.3343	-0.3634
2.0	1.0310	1.0433	0.0077	0.0130	0.2702	-0.3071
3.0	1.0149	1.0188	0.0037	0.0062	0.2402	-0.2602
5.0	1.0058	1.0068	0.0014	0.0021	0.2304	-0.2365
$\lambda_f = 1.00$						
1.1	1.1130	1.4244	0.0240	-0.0110	0.5852	-0.3420
1.5	1.0546	1.0932	0.0116	0.0166	0.2974	-0.3261
2.0	1.0319	1.0463	0.0067	0.0113	0.2411	-0.2767
3.0	1.0152	1.0195	0.0032	0.0054	0.2153	-0.2347
5.0	1.0059	1.0070	0.0012	0.0018	0.2073	-0.2132

Table 7. The effect of a 90-degree material rotation on the stress intensity factors in an orthotropic half-plane stiffened by a single membrane and containing an internal crack; Fig.5, $\theta = 0$, $\{(d - c)/2a\} = 1$, $\lambda_f = (\beta^1_{22}/\beta_{22})(a/h)$, Material 1A, $C_h = 6.8222$.

λ_f	$\frac{d}{a}$	$\frac{k_1(d)}{\sigma_\circ\sqrt{d}}$	$\frac{k_2(d)}{\sigma_\circ\sqrt{d}}$	$\frac{k_2(-2a)}{\sigma_\circ\sqrt{a}}$	$\frac{k_1(d)}{\sigma_\circ\sqrt{d}}$	$\frac{k_2(d)}{\sigma_\circ\sqrt{d}}$	$\frac{k_2(-2a)}{\sigma_\circ\sqrt{a}}$
		$C_h = 6.8222$			$C_h = 3.0358$		
0.0	0.10	1.6923	-0.2201	-0.3535	1.9196	-0.3354	-0.4747
	0.25	1.2998	-0.0973	-0.3169	1.3803	-0.1600	-0.4345
	0.50	1.1138	-0.0356	-0.2411	1.1751	-0.0671	-0.3515
	1.00	1.0704	-0.0005	-0.1253	1.0982	-0.0134	-0.2059
0.2	0.10	1.6568	-0.2078	-0.3386	1.8592	-0.3118	-0.4485
	0.25	1.2492	-0.0916	-0.3051	1.3593	-0.1482	-0.4130
	0.50	1.1114	-0.0336	-0.2333	1.1690	-0.0622	-0.3364
	1.00	1.0702	-0.0005	-0.1221	1.0975	-0.0124	-0.1989
1.0	0.10	1.5480	-0.1701	-0.2923	1.6869	-0.2439	-0.3726
	0.25	1.2159	-0.0742	-0.2677	1.2985	-0.1143	-0.3492
	0.50	1.1035	-0.0272	-0.2081	1.1514	-0.0478	-0.2903
	1.00	1.0695	-0.0004	-0.1115	1.0954	-0.0100	-0.1767

Table 8. Stress intensity factors in an orthotropic half-plane stiffened by a single membrane and containing an edge crack; Fig.1, $\theta = 0$, $c = 0$, $\lambda_f = (\beta^1_{22}/\beta_{22})(a/h)$, Materials 1 and 2.

λ_f	$\frac{d}{a}$	$\frac{k_1(d)}{\sigma_o\sqrt{d}}$	$\frac{k_2(d)}{\sigma_o\sqrt{d}}$	$\frac{k_2(-2a)}{\sigma_o\sqrt{a}}$	$\frac{k_1(d)}{\sigma_o\sqrt{d}}$	$\frac{k_2(d)}{\sigma_o\sqrt{d}}$	$\frac{k_2(-2a)}{\sigma_o\sqrt{a}}$
		$C_h = -1.0944$			$C_h = -1.3137$		
0.0	0.10	2.1371	-0.3809	-0.5481	2.1853	-0.4030	-0.5708
	0.25	1.5102	-0.1818	-0.4938	1.5377	-0.1940	-0.5159
	0.50	1.2592	-0.0742	-0.3941	1.2751	-0.0805	-0.4145
	1.00	1.1585	-0.0110	-0.2030	1.1668	-0.0124	-0.2168
0.2	0.10	2.0570	-0.3508	-0.5140	2.0990	-0.3701	-0.5340
	0.25	1.4814	-0.1670	-0.4666	1.5061	-0.1776	-0.4864
	0.50	1.2509	-0.0684	-0.3760	1.2659	-0.0739	-0.3946
	1.00	1.1578	-0.0102	-0.1964	1.1659	-0.0116	-0.2095
1.0	0.10	1.8369	-0.2678	-0.4190	1.8645	-0.2804	-0.4325
	0.25	1.4006	-0.1256	-0.3883	1.4187	-0.1325	-0.4023
	0.50	1.2270	-0.0517	-0.3216	1.2393	-0.0554	-0.3357
	1.00	1.1556	-0.0008	-0.1757	1.1635	-0.0009	-0.1866

Table 8. Contd., Materials 5 and 6.

λ_f	$\frac{d}{a}$	$\frac{k_1(d)}{\sigma_o\sqrt{d}}$	$\frac{k_2(d)}{\sigma_o\sqrt{d}}$	$\frac{k_2(-2a)}{\sigma_o\sqrt{a}}$	$\frac{k_1(d)}{\sigma_o\sqrt{d}}$	$\frac{k_2(d)}{\sigma_o\sqrt{d}}$	$\frac{k_2(-2a)}{\sigma_o\sqrt{a}}$
		$C_h = 6.8222$			$C_h = 3.0358$		
0.0	0.10	1.4105	-0.0865	-0.2042	1.5155	-0.1121	-0.2443
	0.25	1.1389	-0.0289	-0.1578	1.1889	-0.0400	-0.1941
	0.50	1.0754	-0.0006	-0.0937	1.1017	-0.0008	-0.1194
	1.00	1.0658	0.0000	-0.0219	1.0864	0.0000	-0.0264
0.2	0.10	1.3987	-0.0836	-0.1993	1.4983	-0.1076	-0.2374
	0.25	1.1365	-0.0279	-0.1546	1.1850	-0.0384	-0.1894
	0.50	1.0752	-0.0006	-0.0921	1.1012	-0.0008	-0.1171
	1.00	1.0658	0.0000	-0.0218	1.0865	0.0000	-0.0262
1.0	0.10	1.3586	-0.0733	-0.1824	1.4415	-0.0926	-0.2140
	0.25	1.1284	-0.0244	-0.1433	1.1721	-0.0330	-0.1735
	0.50	1.0742	-0.0005	-0.0865	1.0995	-0.0007	-0.1091
	1.00	1.0658	0.0000	-0.0213	1.0865	0.0000	-0.0257

Table 9. The effect of a 90-degree material rotation on the stress intensity factors in an orthotropic half-plane stiffened by a single membrane and containing an edge crack;Fig.1, $\theta = 0$, $c = 0$, $\lambda_f = (\beta^1_{22}/\beta_{22})(a/h)$, Materials 1A and 2A.

λ_f	$\frac{d}{a}$	$\frac{k_1(d)}{\sigma_o\sqrt{d}}$	$\frac{k_2(-2a)}{\sigma_o\sqrt{a}}$	$\frac{k_1(d)}{\sigma_o\sqrt{d}}$	$\frac{k_2(-2a)}{\sigma_o\sqrt{a}}$	$\frac{k_1(d)}{\sigma_o\sqrt{d}}$	$\frac{k_2(-2a)}{\sigma_o\sqrt{a}}$
		$C_h = 6.8222$		$C_h = 3.0358$		$C_h = 0.0000$	
0.0	0.10	2.4567	-0.3718	2.9870	-0.5085	2.9926	-0.4978
	0.25	1.4614	-0.3236	1.6926	-0.4475	1.7074	-0.4218
	0.50	1.1613	-0.2413	1.2629	-0.3531	1.2809	-0.3195
	1.00	1.0750	-0.1247	1.1099	-0.2051	1.1360	-0.1535
0.2	0.10	2.3702	-0.3545	2.8327	-0.4771	2.8477	-0.4686
	0.25	1.4392	-0.3112	1.6480	-0.4244	1.6666	-0.4014
	0.50	1.1564	-0.2335	1.2510	-0.3379	1.2710	-0.3070
	1.00	1.0746	-0.1216	1.1085	-0.1982	1.1352	-0.1494
1.0	0.10	2.1112	-0.3021	2.4076	-0.3891	2.4418	-0.3852
	0.25	1.3705	-0.2720	1.5200	-0.3564	1.5475	-0.3405
	0.50	1.1409	-0.2083	1.2160	-0.2914	1.2410	-0.2683
	1.00	1.0732	-0.1110	1.1043	-0.1763	1.1330	-0.1357

Table 10. Stress intensity factors in an orthotropic half-plane stiffened by two symmetric membranes and containing an edge crack; Fig.2, $\lambda_f = (\beta_{22}^1/\beta_{22})(a/h)$, Materials 1-3.

λ_f	$\frac{d}{a}$	$\frac{k_1(d)}{\sigma_o\sqrt{d}}$	$\frac{k_2(-2a)}{\sigma_o\sqrt{a}}$	$\frac{k_1(d)}{\sigma_o\sqrt{d}}$	$\frac{k_2(-2a)}{\sigma_o\sqrt{a}}$	$\frac{k_1(d)}{\sigma_o\sqrt{d}}$	$\frac{k_2(-2a)}{\sigma_o\sqrt{a}}$
		$C_h = -0.0022$		$C_h = -1.0944$		$C_h = -1.3137$	
0.0	0.10	2.9899	-0.4882	3.3935	-0.5885	3.5018	-0.6139
	0.25	1.7063	-0.4174	1.8914	-0.5077	1.9418	-0.5310
	0.50	1.2805	-0.3157	1.3697	-0.3951	1.3947	-0.4157
	1.00	1.1359	-0.1522	1.1705	-0.2022	1.1804	-0.2159
0.2	0.10	2.8453	-0.4596	3.1908	-0.5477	3.2821	-0.5697
	0.25	1.6656	-0.3975	1.8310	-0.4787	1.8753	-0.4994
	0.50	1.2705	-0.3037	1.3534	-0.3769	1.3765	-0.3958
	1.00	1.1352	-0.1482	1.1691	-0.1957	1.1787	-0.2088
1.0	0.10	2.4405	-0.3780	2.6537	-0.4378	2.7079	-0.4520
	0.25	1.5469	-0.3378	1.6628	-0.3958	1.6930	-0.4102
	0.50	1.2407	-0.2661	1.3066	-0.3224	1.3244	-0.3367
	1.00	1.1329	-0.1348	1.1649	-0.1752	1.1738	-0.1861

Table 10. Contd., Materials 4-6.

λ_f	$\frac{d}{a}$	$\frac{k_1(d)}{\sigma_o\sqrt{d}}$	$\frac{k_2(-2a)}{\sigma_o\sqrt{a}}$	$\frac{k_1(d)}{\sigma_o\sqrt{d}}$	$\frac{k_2(-2a)}{\sigma_o\sqrt{a}}$	$\frac{k_1(d)}{\sigma_o\sqrt{d}}$	$\frac{k_2(-2a)}{\sigma_o\sqrt{a}}$
		$C_h = 6.8222$		$C_h = 3.0358$		$C_h = -0.0022$	
0.0	0.10	1.7900	-0.2123	1.9944	-0.2551	2.9962	-0.4988
	0.25	1.2115	-0.1585	1.2909	-0.1954	1.7090	-0.4227
	0.50	1.0850	-0.0932	1.1169	-0.1190	1.2816	-0.3204
	1.00	1.0658	-0.0216	1.0865	-0.0264	1.1361	-0.1542
0.2	0.10	1.7639	-0.2069	1.9561	-0.2473	2.8507	-0.4694
	0.25	1.2068	-0.1552	1.2832	-0.1906	1.6680	-0.4022
	0.50	1.0844	-0.0917	1.1158	-0.1167	1.2716	-0.3078
	1.00	1.0658	-0.0215	1.0865	-0.0262	1.1354	-0.1501
1.0	0.10	1.6761	-0.1884	1.8304	-0.2215	2.4437	-0.3858
	0.25	1.1907	-0.1439	1.2574	-0.1745	1.5484	-0.3410
	0.50	1.0825	-0.0862	1.1124	-0.1088	1.2414	-0.2689
	1.00	1.0659	-0.0210	1.0866	-0.0256	1.1331	-0.1363

Table 11. The effect of a 90-degree material rotation on the stress intensity factors in an orthotropic half-plane stiffened by two symmetric membranes and containing an edge crack; Fig.2, $\lambda_f = (\beta^1_{22}/\beta_{22})(a/h)$, Materials 1A-3A.

LIST OF FIGURES

LIST OF TABLES

symmetric membranes and containing an edge crack; Fig.2, $\lambda_f = (\beta_{22}^1/\beta_{22})(a/h)$, Materials 1-6.

Table 11. The effect of a 90-degree material rotation on the stress intensity factors in an orthotropic half-plane stiffened by two symmetric membranes and containing an edge crack; Fig.2, $\lambda_f = (\beta_{22}^1/\beta_{22})(a/h)$, Materials 1A-3A.